Finite-Element Analysis of Microelectromechanical Membranes Vibration

Gailius VANAGAS[1,2]**, Marius MIKOLAJŪNAS**[1,2]**, Viktoras GRIGALIŪNAS**[1]**,
Darius VIRŽONIS**[2*]

[1]*Institute of Physical Electronics, Kaunas University of Technology, Savanoriu 271, LT-50131 Kaunas, Lithuania*
[2]*Department of Electrical Engineering, Panevėžys Institute Faculty of Technologies, Kaunas University of Technology,
Daukanto 12, LT-35212 Panevėžys, Lithuania*

The influence of the capacitive micromachined ultrasound transducers (cMUT) design and operation regimes on the parameters of received signal during the pulse-echo operation was investigated with finite element analysis (FEA). FEA representation of pulse-echo response with electrical signals simulated at the input and output of a model with exploring of conditions of the single cMUT cell operation in immersion was created and experimentally verified. It was found the correlation between the simulated and measured data to be not worse than 0.92. Most of the difference between the data we attribute to post-receive oscillations present in measured signal. Then the influence of the cell design (diameter, vacuum gap size) and operating conditions (excitation pulse amplitude, duration and bias voltage) was explored by simulation. The increase of the pulse/echo effectiveness by increasing of the cell diameter was found. It was further found the negative relationship between the vacuum gap size and the amplitude of the received signal. We also confirm that bias voltage and excitation pulse duration need to be optimized, because the optimization allows creating certain peak performance conditions.
Keywords: capacitive micromachined ultrasound transducer, finite element modeling, pulse-echo characteristics.

1. INTRODUCTION

Electrostatic acoustic transducers are used for excitation and reception of acoustical waves since invention of capacitive microphone in the first half of 20-th century. The principle of operation here is based on vibrations of thin membrane as a result of changed electrostatic field and vice versa. Advancements in silicon micromachining techniques during the last decades created a potential for electrostatic transducers fabricated as micromechanical systems (MEMS). This in turn resulted in possibility of fabricating devices suitable for operation within ultrasound range. The concept of capacitive Micromachined Ultrasound Transducers (cMUT) was created in Standford university [1−3]. It imposes the arrays of hundreds and thousands of micrometer-sized capacitive cells, which are connected in parallel and are operated by electrostatic field as one transducer element. For useful ultrasound range of several megahertz, lateral dimensions of capacitive cells are in the range of tens of microns.

The striking advantage of the electrostatic devices compared to the others types of transducers such as piezoelectric and magnetosstrict is the inherent impedance match between the transducer and the surrounding medium. The low impedance of the membrane is usually negligible. This results in very efficient coupling of the sound waves into and from the sound-bearing medium [4].

The cMUT transducers takes advantages to the well established microelectronic technology, as well as the good mechanical properties of silicon as a basic material for the substrate and the membranes, usually made of silicon nitride. There are ability to integrate electronics on the same silicon wafer where transducers are fabricated. 2D array design can be realized using photolithography techniques.

Actual parameters of structural materials of cMUTs and critical dimensions of the elements of cMUT cells are the main variables determining the basic technical properties of the devices. Therefore it is very important to have an adequate means for calculation and simulation. This work was devoted to analyse and evaluate existing simulation tools and to create the most useful and adequate model for evaluation and analysis of cMUT structure and operation.

2. REVIEW OF EXISTING CALCULATION METHODS

2.1. Static parameters

Capacitive micromachined transducer (Fig. 1) consists of conductive membrane, which can be made of metalized silicon nitride or monocrystalline silicon, vacuum gap, insulating layer and bottom doped silicon bulk which serve as bottom electrode. When a voltage is placed between the metalized membrane and the bulk, Coulomb forces attract the membrane toward the bulk and stress within the membrane resist the attraction. When the membrane is
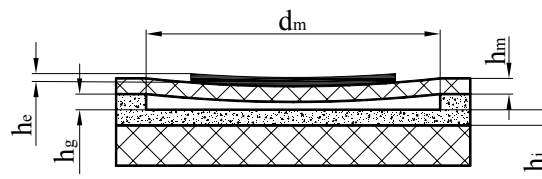
Fig. 1. Cross section of cMUT cell. There h_i − thickness of insulation (silicon dioxide) layer, h_g − vacuum gap height, h_m − thickness of silicon membrane, h_e − thickness of electrode, d_m − diameter for circular cells membranes or length of side for square cells membranes

*Corresponding author. Tel.: +370-45-434247; fax: +370-45-516161.
E-mail address: *darius.virzonis@ktu.lt* (D. Viržonis)

driven by alternating voltage, ultrasound waves are being emitted. Controversially, if the membrane is biased appropriately and subjected to the acoustic waves, significant detection current is generated.

The most important static parameters of cMUT are the membrane displacement performance (static electromechanical transfer function for transmission) and the capacitance performance (static electromechanical transfer function for receiving).

When comparatively thin membrane is fixed at the edges and when the pressure p is applied to it, the displacement of the membrane at any distance r from the membrane center can be calculated by equation (1) from [5]:

$$x = \frac{p}{\sigma_m}\left[\frac{\frac{r_m}{A}[I_0(Ar) - I_0(Ar_m)]}{2I_1(Ar_m)} + \frac{r_m^2 - r^2}{4}\right], \quad (1)$$

$$A = \sqrt{\frac{12\sigma_m(1-v^2)}{(E_m + \sigma_m)h_m^3}}, \quad (2)$$

where E_m is the equivalent value of Young's modulus of metalized membrane, v stands for the value of Poison ratio, σ_m is tension, r_m is membrane radius, h_m is membrane thickness. I_0, I_1 are zero and first order modified Bessel functions respectively.

Electrostatic force applied across the cMUT structure (Fig. 1) when the membrane is curved towards the substrate can be calculated as follows:

$$F_e = \frac{S_m\varepsilon_0 U^2}{2\left(\frac{h_g - x}{\varepsilon_g} + \frac{h_m}{\varepsilon_m} + \frac{h_i}{\varepsilon_i}\right)^2}, \quad (3)$$

where S_m is the membrane area, ε_0 is electric constant ($8.8541878176\times10^{-12}$ F/m), ε_g, ε_m, ε_i – respectively gap, membrane and insulator relative electric constants, U is the bias voltage $x(r)$ stands for equivalent membrane displacement.

The membrane is actuated by the resultant of electrostatic and spring forces. In the static regime can be written:

$$F_e = F_S = pS_m = kx, \quad (4)$$

Where F_S is the membrane resistance to the bending (spring) force, k – the spring constant.

If equations (3) and (4) are put to (1) we get:

$$\frac{4\sigma_m I_1(Ar_m)x}{\frac{2r_m}{A}[I_0(Ar) - I_0(Ar_m)] + I_1(Ar_m)(r_m^2 - r^2)} =$$

$$= \frac{S_m\varepsilon_0 U^2}{2\left(\frac{h_g - x}{\varepsilon_g} + \frac{h_m}{\varepsilon_m} + \frac{h_i}{\varepsilon_i}\right)^2}. \quad (5)$$

Equation (5) can be re-arranged to the equation of 3-rd order and solved in respect of x. Solution is physically feasible only when $h_g > x$. Increase of bias voltage U causes collapse of the membrane, when increase of Coulomb force overcomes an increase of the elastic force. The collapse voltage can be determined as follows [3, 6]:

$$V_{collapse} = \sqrt{\frac{8k\left(\frac{h_g}{\varepsilon_g} + \frac{h_m}{\varepsilon_m} + \frac{h_i}{\varepsilon_i}\right)^3}{27\varepsilon_g S_m}}. \quad (6)$$

Here k is determined from (4) and (1) with boundary condition $r = 0$;

$$k = \frac{4S_m\sigma_m I_1(Ar_m)x}{\frac{2r_m}{A}I_0(Ar_m) + I_1(Ar_m)r_m^2}. \quad (7)$$

Cell capacitance can be determined from the following expression:

$$C(x_{ef}) = \frac{S_m\varepsilon_0}{\left(\frac{h_g - x_{ef}}{\varepsilon_g} + \frac{h_m}{\varepsilon_m} + \frac{h_i}{\varepsilon_i}\right)}. \quad (8)$$

Here x_{ef} is effective displacement of the membrane. Finding x_{ef} is not straightforward, because the curvature of the membrane is complex. Therefore expression (8) is suitable only to find approximate value of the cell capacitance, which is done by dividing the circular membrane to the concentric rings (Fig. 2). In this case cell capacitance:

$$C = \sum_{i=1}^n \frac{S_m^i\varepsilon_0}{\left(\frac{h_g - x_i}{\varepsilon_g} + \frac{h_m}{\varepsilon_m} + \frac{h_i}{\varepsilon_i}\right)}. \quad (9)$$

Here S_m^i is an area of i-th ring; x_i is a shift of the ring within r_i from the membrane center. It is determined by equation (1) or (5). Analytical methods [7] and Finite Element Analysis [8] are used to determine the curvature of the membrane.
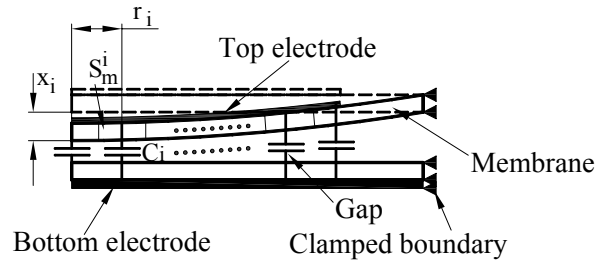

Fig. 2. Segmented membrane

For calculation the capacitance, we are using one of the outputs of the FEM model for the displacement: the cumulative energy in CMUT capacitor E_C [9], which then is converted to capacitance, using a following fundamental equation:

$$C = \frac{2E_C}{U^2}. \quad (10)$$

This method to find the capacitance is advantageous over the methods published [8], because it does not involve any additional segmentation of the membrane.

2.2. Mechanical Impedance of a Membrane

For stretched circular membrane with tension and stiffness differential equation of motion satisfied by every point on surface can be written as [5, 3]:

$$\frac{(E_m + \sigma_m)h_m^3}{2\sigma_m(1-v^2)}\nabla^4 x - \sigma_m \nabla^2 x - p - \omega^2 \rho h_m x = 0 , \qquad (11)$$

where ∇x is a gradient of x.

Solution of displacement:

$$x = \frac{p}{\omega^2 \rho h_m}\left[\frac{k_2 I_1(k_2 r_m)J_0(k_1 r) + k_1 J_1(k_1 r_m)I_0(k_2 r)}{J_0(k_1 r_m)k_2 I_1(k_2 r_m) + k_1 J_1(k_1 r_m)I_0(k_2 r)} - 1\right], (12)$$

where:

$$k_1 = \sqrt{\frac{\sqrt{d^2 + 4c\omega^2} - d}{2c}} \; ; \; k_2 = \sqrt{\frac{\sqrt{d^2 + 4c\omega^2} + d}{2c}} \; ;$$

$$c = \frac{(E_m + \sigma_m)h_m^2}{h_m^3 12\sigma_m(1-v^2)} \; ; \; d = \frac{\sigma_m}{\rho h_m} \; .$$

J_0, J_1 are zero and first order Bessel functions respectively.

Vibrating membrane motional velocity V:

$$V = j2\pi\omega\int_0^{r_m} rx dr =$$

$$= \frac{jpS_m}{\omega\rho h_m}\left[\frac{\frac{2}{a}\left(\frac{k_2}{k_1} + \frac{k_1}{k_2}\right)I_1(k_2 r_m)J_1(k_1 r_m)}{J_0(k_1 r_m)k_2 I_1(k_2 r_m) + k_1 J_1(k_1 r_m)k_2 I_0(k_2 r_m)} - 1\right]. \quad (13)$$

The impedance of the membrane, being p/V is

$$Z_m = \frac{p}{V} =$$

$$= \frac{j\omega\rho h_m}{S_m}\left[\frac{\left[k_2 \frac{J_0(k_1 r_m)}{J_1(k_1 r_m)} + k_1 \frac{I_0(k_2 r_m)}{I_1(k_2 r_m)}\right]\frac{k_1 k_2 r_m}{2(k_1^2 + k_2^2)}}{\left[k_2 \frac{J_0(k_1 r_m)}{J_1(k_1 r_m)} + k_1 \frac{I_0(k_2 r_m)}{I_1(k_2 r_m)}\right]\frac{k_1 k_2 r_m}{2(k_1^2 + k_2^2)} - 1}\right]. \quad (14)$$

Equivalent circuit method proposed by Mason [5] is also suitable for harmonic analysis of cMUT. By introducing the value of mechanical impedance to the equivalent circuit one can determine analytically the properties of a transducer coupled with a sound propagation environment. In the equivalent circuit shown in Fig. 3 (taken form [3] and [4]) Z_m is the complex mechanical impedance of the cMUT, Z is the acoustical impedance of the surrounding medium.
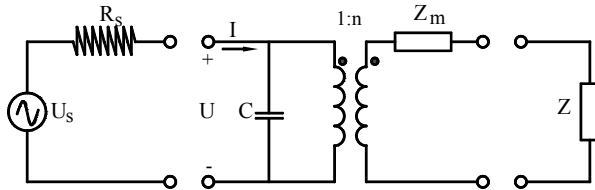

Fig. 3. Electrical equivalent circuit of cMUT

Transformer represents the electromechanical conversation between the electrical and the acoustical ports. Which is [4]:

$$n = U\frac{\varepsilon_0 S_m}{(h_{ef} - x)^2} \; . \qquad (15)$$

Where h_{ef} is the effective gap height evaluating insulating layer and membrane thickness and material. U

stands for the bias voltage. It is obvious from (15) that for high n the gap must to be possibly small.

For rapid evaluation of critical cMUT dimensions the software, based on the above described theory, was elaborated in MATLAB environment.

If coupling to the ultrasound propagation medium of the membranes with complex structure is to be evaluated with the need to obtain precise results, Finite Element Analysis (FEA) is used and successfully applied to determine various functional properties of cMUT.

For instance [6], [7] static FEA of membrane deflection is done; in [8] and [10] harmonic analysis is used; [11] and [13] are investigating non-linear regimes of cMUT operation. Transient analysis used in our investigation is described in this paper.

For verification of FEA results acoustical pressure of a real transducer in transmit regime is measured or the movements of a membrane are measured with a real-time optical interferometry [8]. In practice the most common and the most informative method of testing the entire ultrasound transmit/receive channel is the pulse-echo response measurement [12]. The experimental setup for pulse – echo response measurement is composed of transmit/receive block, connected to the cMUT, pulse generator and oscilloscope (Fig. 4). The transmit/receive block supplies the rectangular pulses with adjustable due, which can be optimized for maximum transmit/receive reliability. During the transmit cycle the pulse is directed to cMUT via the signal separation circuit. During the receive cycle the same signal separation circuit directs the pulse from cMUT to the amplifier.
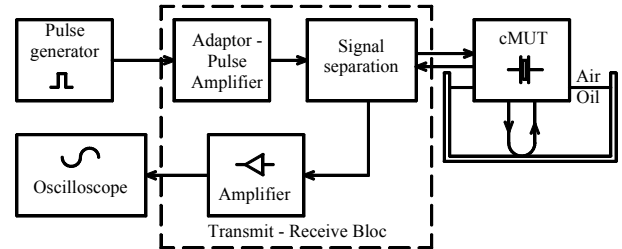

Fig. 4. Pulse – echo experiment schematic

3. METHODS OF CALCULATION USED

In our work commercially available FEA software (ANSYS) was used. The 2D model was chosen for simulation time economy. The single capacitive ultrasound transducer (cMUT) cell, immersed in fluid (Fig. 5) was simulated. The membrane and electrode were divided by PLANE42 elements, and the vacuum gap was divided by TANS126 elements. The ambient medium was modeled as hemisphere, consisting of FLUID29, with FLUID129 at the hemisphere edge. The last was introduced to prevent the ultrasound reflections from the medium boundary. For completeness of the results, a top electrode of cMUT cell was also included in the model. The acoustic mirror was positioned at the distance of $L = 0.4$ mm from cMUT active surface for reflection of acoustic waves; it was divided by PLANE42 elements. The same cMUT cell was used for ultrasound excitation and reception. The distance between the active surface of cMUT and the acoustical mirror was chosen so that the period of the time of acoustic

pulse travel in both directions would be sufficient to distinguish between excited and reflected pulses. On the other hand, the distance between the active surface of cMUT and the mirror is limited by the reasonable calculation time.

Membrane and electrode were divided in rectangular elements of 2 μm. This is nearly optimal element dimension, if the lateral size of the cell is tens of microns. The size of ultrasound propagation medium divisions is limited by the wavelength of the sound wave: for representative results with uncertainty less than 3 %, as much as 10 elements are supposed to fit within the one wavelength. On the other hand, any distortions of the ultrasound propagation medium caused by differently-sized elements would cause the model to generate undesired (non-informative) reflections. So the ultrasound propagation medium was divided in 2 μm elements, and this limited the maximum of frequencies available for analysis to 75 MHz ($\lambda = 0.02$ mm for the speed of sound in water $c = 1500$). The time-domain FEA with digitizing period of 1.3 ns was applied to simulate the pressure front. Following dimensions were taken: membrane thickness $h_m = 1.5$ μm, vacuum gap $h_g = 0.15$ μm, insulation layer thickness $h_i = 0.3$ μm, aluminum electrode thickness $h_e = 0.4$ μm. The cMUT cell lateral size was taken 39, 40 and 44 μm of circular and rectangular shape.
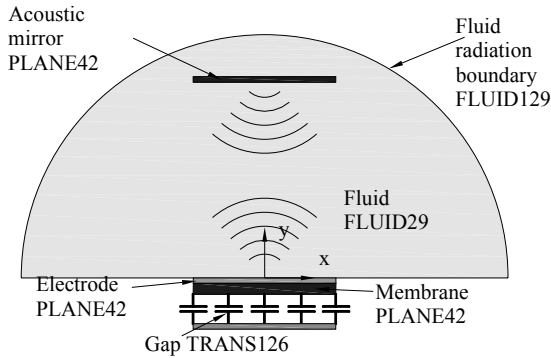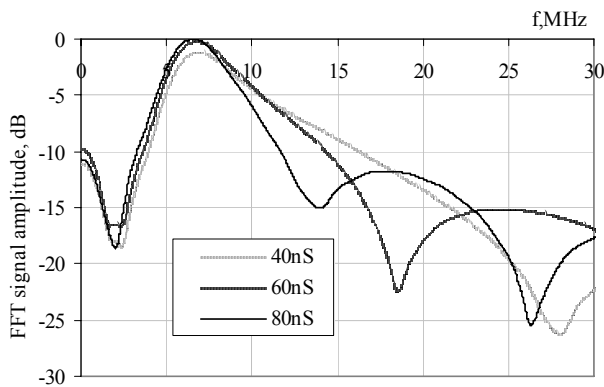

Fig. 5. Structure of the FEM model

Fig. 6. Calculated dependence echo signal to pulse duration. $d_m = 39$ μm, $h_g = 0.15$ μm, $h_i = 0.3$ μm, $h_e = 0.4$ μm, $V_{bias} = 0.8 V_{collapse}$, $V_{pulse} = 60$ V, $V_{collapse} = 115$ V

Excited ultrasound pulse is propagating over the medium from the cMUT surface; then it is reflected by the mirror and travels back to the membrane. When the pressure front of reflected pulse approaches the membrane, it is standing still (the movement caused by the short

electrical pulse is finished). When the pressure front reaches the membrane, it causes membrane to move, thus hanging the capacitance of the cell. The change of a capacitance changes the conditions of the electrical energy, which is stored in a cell, and this induces the current, which can be calculated as follows:

$$I = \frac{dQ}{dt} = \frac{d}{dt}(C(t)U(t)). \tag{16}$$

Here Q is electrical charge accumulated by the cMUT cell.

4. MODELING RESULTS

By using FEA the changes in energy accumulated by cMUT cell and membrane displacement were calculated. Afterwards, using equations (10) and (16), we calculated the values of the received and transmitted signals. The water was supposed to be the ultrasound propagation medium when simulated; main parameters of structural materials used in the model are shown in Table 1.

Bias voltage was set to 80 % of collapse voltage. Ultrasound wave was excited by rectangular 60 ns long pulse of 60 V. Pulse due was chosen to maximize the amplitude of the received pulse and minimize distortions. Several cases of received pulse frequency spectra for different excitation pulse dues are shown in Fig. 6. In Fig. 7 simulated movement of a membrane's central point is shown both during transmit and receive phase.

Table 1. Main parameters of materials used in the FEA model

Materials properties [14]	Si	Si₃N₄	Al
Elasticity modulus, GPa	148	200	68
Poisson coefficient	0.17	0.24	0.35
Density, kg/m³	2329	3187	2699

Verification of a model was performed with a cMUT cells produced with wafer bonding technique [16] and having 39 μm diameter circular membranes. For pulse-echo experiment we used experimental setup shown in Fig. 4. We used function/arbitrary waveform generator Agilent 33220A for excitation pulses. Received echo signal was captured using oscilloscope Tektronix TDS2024. CMUT was immersed in high quality transformer oil NESTE TRAFO 10X. Density of the oil is 895 kg/m³ and the disruption voltage of it is 52 kV. The interface between the upper side of the oil container bottom and the oil was used as an acoustical mirror to reflect the pulse back to the transducer. This interface was 5 mm away from the transducer surface. The thickness of the plexiglas container bottom was made to be 10 mm in order to have the clear separation between the pulses reflected from the oil–plexiglas interface and the bottom surface of the container. Unipolar pulse excitation was used to obtain the frequency response of cMUT. An array of circular membranes having dimensions of (300×5000) μm was operated.

Frequency response diagrams for calculated and measured results were obtained using Fast Fourier Transform (FFT).

Calculated and measured receive signals were normalized and put in a single diagram on Fig. 8 for comparison. The correlation coefficient between simulated and

measured data is as much as 0.92. The main difference between simulated and measured signals is post-receive oscillations in measured signal, which is attributable to the transverse waves through the cMUT surface structure and silicon substrate [5].
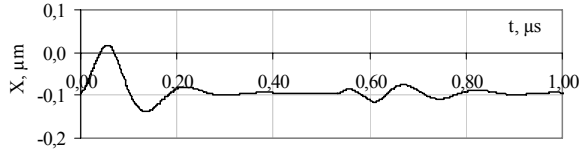

Fig. 7. Calculated pulse – echo displacement results for central point of circular membrane. $d_m = 39$ µm, $h_g = 0.15$ µm, $h_i = 0.3$ µm, $h_e = 0.4$ µm, $V_{bias} = 0.8 V_{collapse}$, $V_{pulse} = 60$ V, $t_{pulse} = 60$ ns
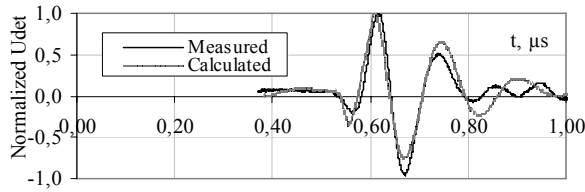
Fig. 8. Measured and calculated normalized echo signal for circular membrane. $d_m = 39$ µm, $h_g = 0.15$ µm, $h_i = 0.3$ µm, $h_e = 0.4$ µm, $V_{bias} = 0.8 V_{collapse}$, $V_{pulse} = 60$ V, $t_{pulse} = 60$ ns

The amplitude of received signal has strong positive dependence on the bias voltage: it increases with increase of DC voltage. Fig. 9 shows calculated and experimental frequency response of cMUT biased 80 % and 60 % from collapse voltage. The central frequency shifts with increasing bias voltage to lower frequencies. Fig. 10 shows results of investigating the impact of the vacuum gap size to the amplitude of received pulse. For effective operation cMUT cells are usually biased close to their collapse voltages. Reducing the gap height reduces the collapse voltage.
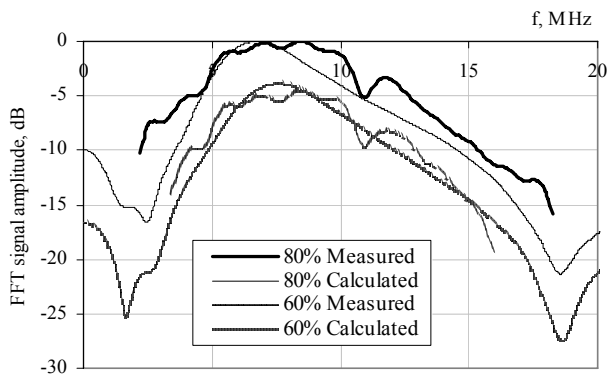

Fig. 9. Measured and calculated frequency response of cMUT biased 80 % and 60 % from collapse voltage for circular membrane. $d_m = 39$ µm, $h_g = 0.15$ µm, $h_i = 0.3$ µm, $h_e = 0.4$ µm, $V_{collapse} = 115$ V, $V_{pulse} = 60$ V, $t_{pulse} = 60$ ns

Therefore the bias voltage was not kept constant in this investigation, but instead always set to 80 % of the collapse voltage. When the vacuum gap height is decreasing, the amplitude of simulated received signal is increasing, if other conditions are kept adequately the same. In respect of 0.1 µm gap, which was supposed to have zero attenuation, 0.15 µm vacuum gap dropped signal to –0.95 dB, 0.2 µm gap attenuate to –2.5 dB, 0.3 µm gap

attenuate to –5.5 dB. Impact of the membrane diameter to the received signal is shown in Fig. 11. It can be concluded that not only the shift of the central frequency towards lower frequencies occurs when the cell diameter is increased, but also larger membranes are more effective: the amplitude of received signal is larger. If 44 µm diameter membrane is supposed to be at 0 attenuation
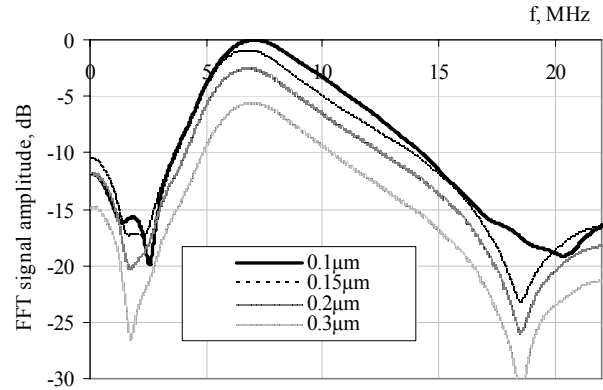

Fig. 10. Calculated dependence of echo signal on the vacuum gap size. cMUT is biased at 80 % from the collapse voltage in all cases. Circular membrane $d_m = 40$ µm, $h_g = 0.1$, 0.15, 0.2, 0.3 µm, $h_i = 0.3$ µm, $h_e = 0.4$ µm, $V_{collapse} = 68$, 115, 167, 276 V accordingly $V_{pulse} = 40$ V, $t_{pulse} = 60$ ns
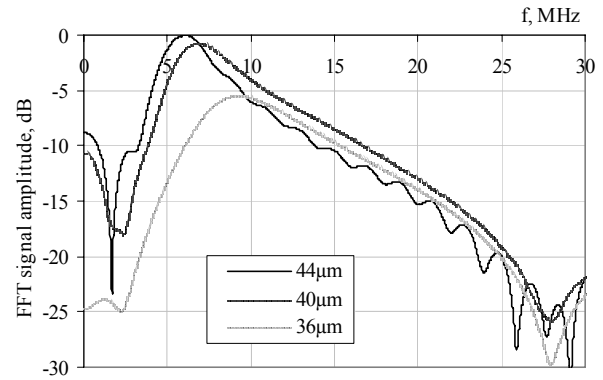

Fig. 11. Calculated dependence echo signal to the membrane diameter. cMUT biased 80 % from collapse voltage for circular membrane. $d_m = 44$, 40, 36 µm, $h_g = 0.15$ µm, $h_i = 0.3$ µm, $h_e = 0.4$ µm, $V_{collapse} = 95$, 115, 143 V accordingly $V_{pulse} = 40$ V, $t_{pulse} = 40$ ns

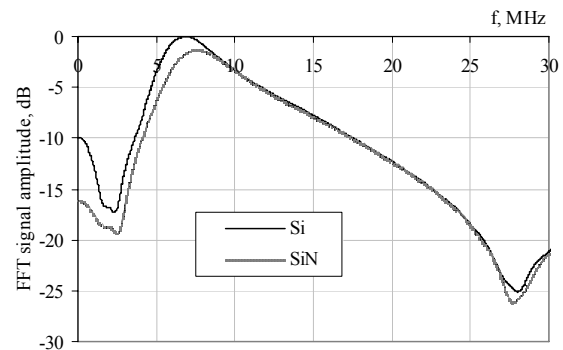**Fig. 12.** Calculated dependence echo to the membrane material. CMUT biased 80 % from collapse voltage for circular membrane. $d_m = 40$ µm, $h_g = 0.15$ µm, $h_i = 0.3$ µm, $h_e = 0.4$ µm, $V_{collapse} = 115$ V for Si membrane and $V_{collapse} = 130$ V, for Si_3N_4 membrane $V_{pulse} = 40$ V, $t_{pulse} = 60$ ns

level, 40 μm diameter membrane attenuates the signal at –0.73 dB level, 36 μm membrane correspondingly to 5.48 dB, when the characteristics of excitation pulse and all other conditions Central frequency increase from 6.06 MHz for 44 μm membrane to 6.86 MHz for 40 μm membrane and 9.32 MHz for 36 μm membrane.

In Fig. 12 the frequency response of the same cMUT cell having membrane of silicon and silicon nitride is compared. Thanks to lower density, lower elasticity and Poisson ratio the cell with membrane of monocrystalline silicon has 1.34 dB higher amplitude of received signal than the same cell having silicon nitride membrane. Central frequency for silicon nitride membrane is 7.55 MHz and 6.86 MHz for silicon membrane.

CONCLUSIONS

Described method of cMUT operation analysis, in contrast with the earlier published works, allows effective and comparatively simple evaluation of design-related electromechanical performance of cMUT transducer. It also is suitable for exploring the impact of variation of the properties of structural materials. The adequacy of a method was proven by the experimental verification.

The correlation coefficient of simulated and experimentally captured echo pulse was found to be not less than 0.92. As the model does not simulate transverse acoustical waves, which possibly occur in reality, this was the main difference with the captured signal. This shows the great adequacy of the model and its ability to present the results with practical significance.

The method, described in this paper, is suitable for modeling of physical signals having low and high amplitudes, exploring non-linear regimes of cMUT operation, for example, operation in collapse regime.

It was determined that increasing of the vacuum gap decreases the efficiency of transducer operation, because the amplitude of received signal decreases. If the vacuum gap is increased from 0.1 μm to 0.15 μm the received signal is attenuated to –0.95 dB; when the gap is increased to 0.2 μm, attenuation increase to –2.5 dB; if the vacuum gap is increased to 0.3 μm, received signal is attenuated to –5.5 dB. These observations determine the conditions for the surface roughness of the bottom of etched cavity: at practical minimum of vacuum gap height of 150 nm, maximal allowable cavity bottom surface roughness is 15 nm (10 % level), which calls for R_a (common parameter of surface roughness) to be estimated less than 15 nm.

It was also concluded that decrease of the membrane radius not only causes the increase of the central frequency, but also attenuates the received signal. When the radius of a membrane is decreased from 44 μm to 40 μm, the received signal attenuates for –0.73 dB; if the membrane radius is decreased to 36 μm, attenuation is at –5.48 dB level. At the same time central frequency from 6.06 MHz for 44 μm membrane increases to 6.86 MHz for 40 μm membrane and to 9.32 MHz for 36 μm diameter membrane.

Using the described calculation method the influence of membrane material properties to echoed signal parameters can be evaluated. As an example, cMUT cell having silicon membrane has 1.34 dB higher amplitude of received signal than the same cell having silicon nitride membrane.

REFERENCES

1. **Haller, M. I., Khuri-Yakub, B. T.** A Surface Micromachined Electrostatic Ultrasonic Air Transducers *Ultrasonics, Ferroelectrics and Frequency Control, IEEE Transactions on*: 43 1996: pp. 1–6.
2. **Soh, H. T., Ladabaum, I., Atalar, A., Quate, C. F., Khuri-Yakub, B. T**. Silicon Micromachined Ultrasonic Immersion Transducers *Appl. Phys. Lett.* 69 1996: pp. 3674–3676.
3. **Ladabaum, I., Jin, X., Soh, H. T., Atalar, A., Khuri-Yakub, B. T.** Surface Micromachined Capacitive Ultrasonic Transducers *Ultrasonics, Ferroelectrics and Frequency Control, IEEE Transactions on* 1998 45 pp. 678–690.
4. **Ergun, A. S., Yaralioglu, G. G., Khuri-Yakub, B. T.** Capacitive Micromachined Ultrasonic Transducers: Theory and Technology *Journal of Aerospace Engineering* 16 (2) 2003.
5. **Mason, W. P.** Electromechanical Transducers and Wave Filters. New York: Van Nostrand, 1948.
6. **Bozkurt, A., Ladabaum, I., Atalar, A., Khuri-Yakub, B. T.** Theory and Analysis of Electrode Size Optimization for Capacitive Microfabricated Ultrasonic Transducers *Ultrasonics, Ferroelectrics and Frequency Control, IEEE Transactions on* 1999 46 pp. 1364–1374.
7. **Nikoozadeh, A., Bayram, B., Yaralioglu, G. G., Khuri-Yakub, B. T.** Analytical Calculation of Collapse Voltage of CMUT Membrane *Ultrasonics Symposium* 1 2004: pp. 256–259.
8. **Yaralioglu, G. G., Ergun, S. A., Khuri-Yakub, B. T.** Finite-element Analysis of Capacitive Micromachined Ultrasonic Transducers *Ultrasonics, Ferroelectrics and Frequency Control, IEEE Transactions on* 2005 52 pp. 2185–2198.
9. **Vanagas, G., Mikolajūnas, M., Grigaliūnas, V, Jarimavičiūtė-Žvalionienė, R., Ivašauskas, A., Viržonis, D.** Investigation of Dynamic Parameters of Multilayered Microelectromechanical Membranes with Finite Element Modelling *Materials Science* (*Medžiagotyra*) 14 (2) 2008: pp. 175–178
10. **Yaralioglu, G. G., Bayram, B., Nikoozadeh, A., Khuri-Yakub, B. T.** Finite Element Modeling of Capacitive Micromachined Ultrasonic Transducers *Medical Imaging* 2005 Proc. of SPIE Vol. 5750.
11. **Bayram B., Goksen G., Yaralioglu G. G., Krupnik M., Ergun A. S., Khuri-Yakub B. T.** Dynamic Analysis of Capacitive Micromachined Ultrasonic Transducers. *Ultrasonics, Ferroelectrics and Frequency Control, IEEE Transactions on* 2005 No.12
12. **Vanagas, G., Mikolajūnas, M., Viržonis, D.** Testing the Capacitive Micromachined Transducers Produced with Wafer Bonding Process *ITELMS'2008: Proceedings of the 3rd International Workshop* 2008: pp. 132–139.
13. **Roh, Y., Khuri-Yakub, B. T.** Finite Element Analysis Of Underwater Capacitor Micromachined Ultrasonic Transducers *Ultrasonics, Ferroelectrics and Frequency Control, IEEE Transactions on* 2002 49 pp. 293–298.
14. **Shackelford, J. F., Alexander, W.** Materials Science and Engineering Handbook. CRC Press LLC, 2001.
15. **Wojcik, G., Mould, J., Reynolds, P., Fitzgerald, A., Wagner, P., Ladabaum, I.**. Time-domain Models of MUT Array Crosstalk in Silicon Substrates *Ultrasonics Symposium* 1 2000: pp. 909–914
16. **Ergun, A. S., Huang, Y., Zhuang, X., Oralkan, O., Yaralioglu, G. G., Khuri-Yakub, B. T.** Capacitive Micromachined Ultrasonic Transducers: Fabrication Technology *IEEE Transactions on Ultrasonic, Ferroelectrics and Frequency Control* 52 (12) December 2005.